High-Resolution Images of Defects in Liquid Crystalline Polymers in the Smectic and Crystalline Phases

I. G. Voigt-Martin* and H. Durst

Institut für Physikalische Chemie, Universität Mainz, D-6500 Mainz, Welder Weg 15, West Germany. *Received December 23, 1987*

ABSTRACT: Electron diffraction and high-resolution imaging techniques have been used in order to obtain structural information about smectic planes in liquid crystalline polymers in the smectic phase and about lattice planes in the crystalline phase. Discrepancies between the long spacings observed by electron diffraction and the distance between mesogenic units on the fully extended main chain are discussed, and possible models are proposed. The purpose of this work was to investigate the defects which can occur in such systems. Multiple dislocations were observed in the smectic planes of liquid crystalline polymers, whereas only single dislocations appeared in the lattice planes of crystalline material.

Introduction

In order to elucidate the structure of the smectic planes in liquid crystal polymers, a polymer was chosen which was available with slightly different molecular architectures. In this case, identical mesogenic groups, which are responsible for liquid crystal formation, where situated (a) in the polymer main chain as well as in the side group, (b) in the polymer main chain only, and (c) in the side group only.

Electron diffraction patterns of the three systems were compared in order to obtain a better understanding of their structure. However, structural details concerning defects in these planes can be reliably obtained only by direct imaging. For this reason, high-resolution techniques were applied to these highly sensitive samples in order to observe the smectic planes directly in real space.

Sample Preparation

The main-chain/side-group liquid crystalline polymer investigated here is a polymalonate with azobenzene as the mesogenic groups in the main chain and cyanoazobenzene as the mesogenic side groups. Its synthesis has been described elsewhere.[1] The chemical constitution and geometry of the molecule is indicated below.

main-chain repeating unit length = 35 Å

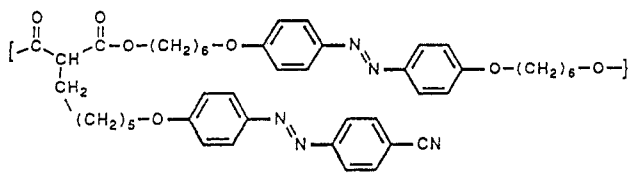

side-chain length, 24 Å

Thin films were prepared by solution casting as described previously[2] using a 0.1% solution in chloroform. By surface tension effects, a certain amount of prealignment was achieved. Subsequent annealing of the thin film close to the smectic–isotropic transition temperature caused orientation of the mesogenic groups.[3] By surface replication and shadowing, these films are shown to be about 200 Å thick.

High-Resolution Electron Microscopy

The term "high resolution" is not strictly appropriate when atomic planes having a spacing more than 20 Å are to be imaged. However, the technique of phase contrast imaging which has to be used in this case is identical with that for imaging atomic planes having spacings less than 5 Å with a few additional complications. This is obvious when we consider the properties of the electron microscope transfer function. The object transform is

$$T^{o}(\alpha,\theta) = \int\int \sigma(x,y) \exp\left\{-\left[\frac{2\pi i}{\lambda}\right][x\alpha\cos\theta + y\alpha\sin\theta]\right\} dx\, dy$$

where $\sigma(x,y)$ is the projected density in atoms per unit area at object plane coordinates x,y, $\alpha = 2\sin\theta$ is the scattering angle, λ is the electron wavelength, and θ is the azimuthal coordinate.[4] Spherical aberration, C_s, and defocus, Δf, of the objective lens lead to a phase shift, $\chi(\alpha)$, that the scattered wave undergoes at the diffraction plane of the objective lens, given by

$$\chi(\alpha) = \frac{2\pi}{\lambda}\left[-\frac{1}{4}C_s\alpha^4 + \frac{1}{2}\Delta f\alpha^2\right]$$

$\sin\chi$ for the Philips EM 420 used in this investigation is shown in Figure 1. For a defocus value $\Delta f = 0$, there is no phase contrast, so we cannot expect to image lattice planes. For a defocus value at 1000 Å, the transfer function behaves well above 5×10^{-2} Å^{-1}, i.e., for small atomic distances. Unfortunately large atomic distances above 20 Å lie in the angular range below 0.05 Å^{-1}, where there is very little phase contrast but considerable amplitude contrast. Figure 1 shows that the phase contrast function increases faster at small angles with increasing defocus value, Δf. For optimum imaging of planes between 20 and 30 Å, the defocus value ranges from 5000 to 10 000 Å. Increasing the defocus value leads to some improvement in the small-angle range, but the function oscillates badly at higher angles. Consequently, the images of smectic planes are not very sharp and are disturbed by unpleasant noise effects. Therefore, the micrographs shown in this paper appear out of focus and rather granular. However, the planes are clearly detectable in the original micrographs, and copies of the transparent overlays appear beside many of the originals in order to aid the reader in interpretation.

The extinction distance for these polymers was calculated to be about 1000 Å. In order to obtain this value, we approximated the packing of the side chains containing the mesogenic groups with an orthorhombic cell. Using that cell, all the positions of the atoms were estimated. With the usual expressions for the structure factors and the scattering amplitudes for electrons from the *International Tables of Crystallography III*, a computer program was applied in order to calculate the extinction distances. Consequently, these films of thickness ~200 Å are thin enough to neglect multiple scattering in image interpretation. The samples are extremely beam sensitive, so all the precautions regarding low dose, low temperature specimen drift, and astigmatism described previously[5] apply here as well.

0024-9297/89/2222-0168$01.50/0

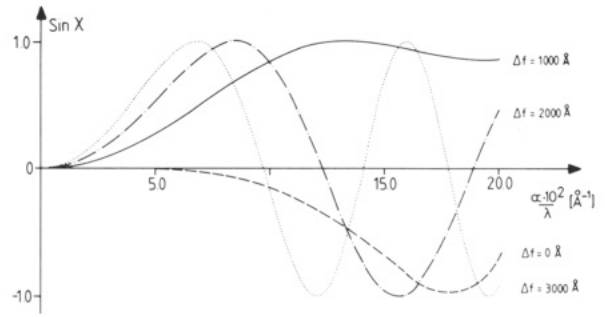

Figure 1. Phase contrast transfer function for Philips EM 420 at 100 kV for different values of defocus. ($\alpha = 2 \sin \theta$, $\chi(\alpha) = (2\pi/\lambda)[-(1/4)C_s\alpha + (1/2)\Delta f\alpha^2]$, $C_s = 2$ mm, $\lambda = 0.037$ Å).

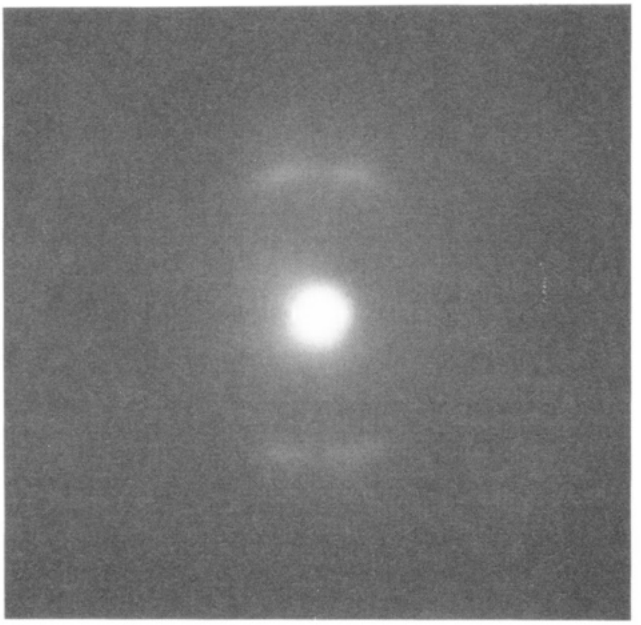

Figure 2. Electron diffraction pattern from main-chain/side-group polymalonate.

Orientation and Structure of Smectic Planes in Thin Films

Some bright field and dark field effects observed in electron microscopy have been described previously.[2,3,5] A typical diffraction pattern for the smectic phase of the main-chain/side-group polymalonate is shown in Figure 2. There are sharp small-angle diffraction maxima with 2–3 higher orders indicating the director direction n and broad halos in the perpendicular direction. The conclusions from those investigations which are relevant for this paper were that in these thin films, elongated, approximately parallel-oriented regions are formed, where the smectic planes are perpendicular to the long axis of the oriented regions and the mesogenic groups generally *lie in the plane of the film* (i.e., the smectic planes are perpendicular to the plane of the film).[1] The smectic planes were shown to be curved. As the extent of the smectic regions increased, the elongated regions merged and the curvature of the smectic planes was shown to develop into an undulation. The oriented halos observed in the diffraction pattern indicated considerable disorder perpendicular to the smectic planes. The sharp small-angle diffraction maxima indicating the smectic order always give a long spacing ($L = 26$ Å) which is considerably smaller than the distance, d, between the mesogenic units on the main chain (35 Å). Possible models to account for this are depicted in Figure 3, with the appropriate diffraction patterns. The model diffraction patterns also indicate the

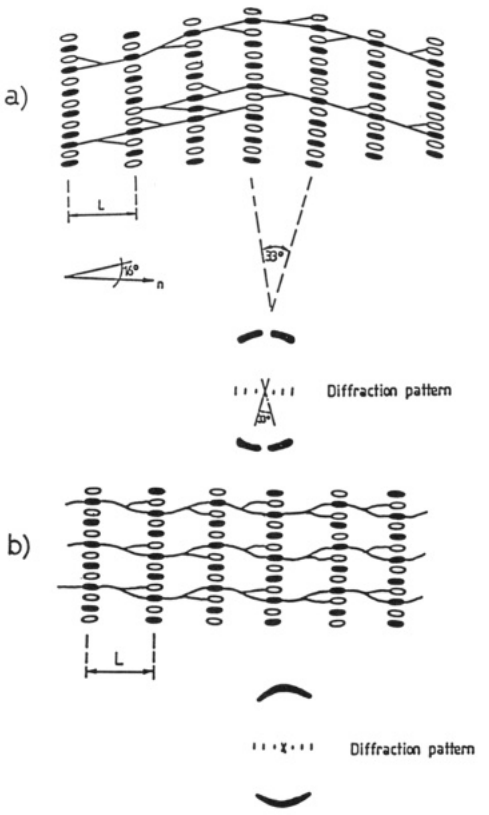

Figure 3. Possible molecular models with appropriate diffraction patterns to account for observed long spacing.

amorphous oriented halos arising from the liquidlike order between mesogenic units. As the electron diffraction pattern in Figure 2 indicates, we generally observe the split halo enclosing an angle of 33° in thin films of these materials under the annealing conditions used here, so model (a) is appropriate in this case. However, this angle is not sufficient to account for such a large difference between L and d, so the main chain is clearly not in all-trans conformation.[1] This makes sense because the bend in the main chain has to be accounted for as well as the bend into the third dimension, which cannot be adequately represented in the diagram. The path of the *polymer chain* is not uniquely determined. While the preferred orientation of the mesogenic groups is determined by the diffraction pattern, the trajectory of the individual polymer chain is expected to form loops or bend down into the third dimension perpendicular to the plane of the film.

Formation of Smectic Planes

When the orientation as observed by electron diffraction (reciprocal space) initially develops after short annealing times, the microscope is adjusted in the manner described previously for image formation.[5] Figure 4 shows the image typically observed after short annealing times. The oriented regions are long in the A direction and short in the B direction. It can be seen that the smectic planes are curved from the beginning. In some cases it is clear that an undulation is beginning to develop. There are no defects in these short sections. Between the highly oriented regions with smectic planes precisely perpendicular to the plane of the film (thick lines in the transparent overlay), the electron micrographs indicate a high level of graininess (i.e., noise). However, careful inspection indicates some preferred orientation in these regions (thin lines in the transparent overlay) such that the highly oriented bands could be connected. In principle such loss of contrast has many potential sources: (1) extra or deficient smectic

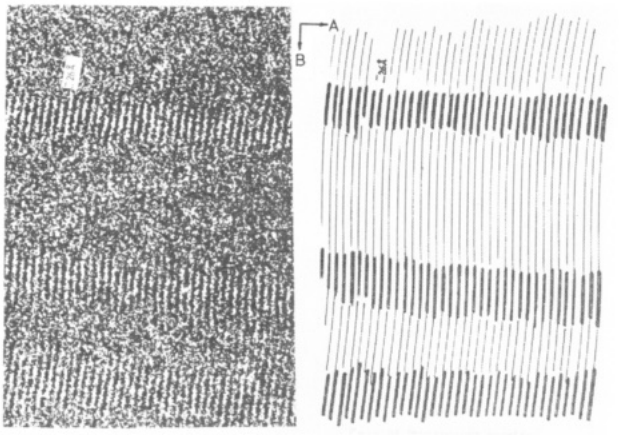

Figure 4. High-resolution image of a main-chain/side-group liquid crystalline polymalonate showing smectic layers after short annealing time.

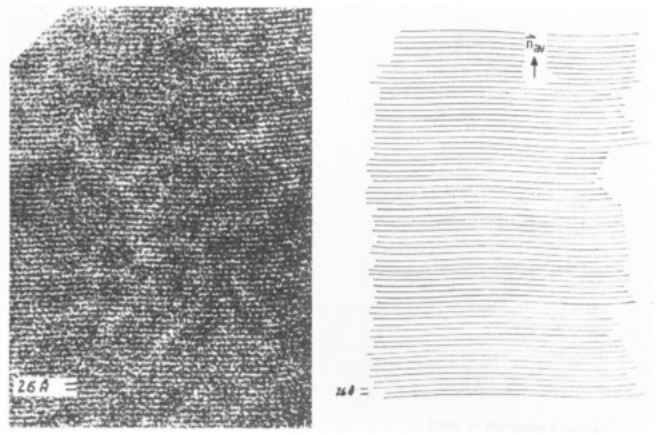

Figure 5. High-resolution image of a main-chain/side-group liquid crystalline polymalonate showing smectic layers after long annealing time.

layers, (2) sample tilt from film undulations, (3) radiation damaged area, (4) nonordered region (nematic), and (5) defect strain field causing strong deviation from the Bragg condition.

After longer annealing times, the whole sample becomes virtually fully oriented, suggesting that cause 3 is not responsible. Careful analysis of these regions using correlation techniques and Fourier filtering[10] show that there is less perfect orientation in these regions which is hidden by the noise in the electron micrographs. This is strong evidence for (1).

The smectic planes on all micrographs show undulations with a wavelength $\lambda \sim 0.1$ μm and an amplitude of about 26 Å. These undulations were never observed in crystalline samples.

Formation of Defects

After the same orientation is developed throughout the sample, the smectic planes do not always come into perfect register and dislocations are formed. The dislocations observed so far are edge dislocations with a burgers vector **b** corresponding to one atomic spacing or a multiple of this number. They are marked by a D in the micrographs. By far the most commonly occurring case is the simple dislocation (Figure 6). In the case shown here, we observe one additional smectic plane going into the defect. In the future discussion, we shall refer to such a defect as a 1:0 dislocation. The interatomic distances remain unchanged, but there is a distortion of the adjacent planes in the immediate vicinity of the defect.

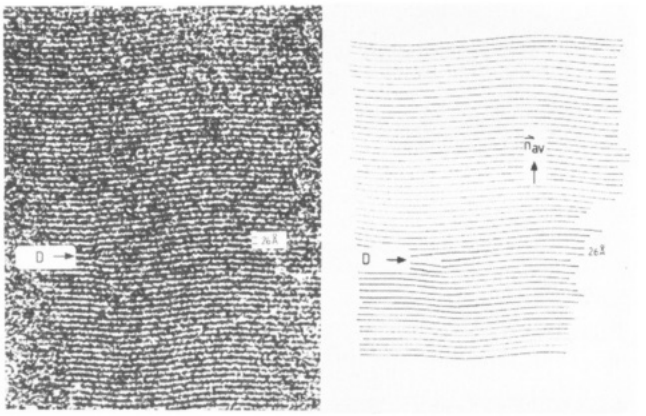

Figure 6. High-resolution image of a main-chain/side-group liquid crystalline polymalonate showing edge dislocation (1:0).

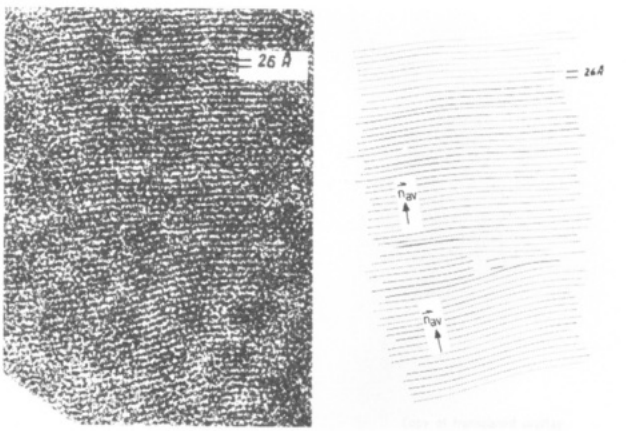

Figure 7. High-resolution image of a main-chain/side-group liquid crystalline polymalonate showing edge dislocation (4:2).

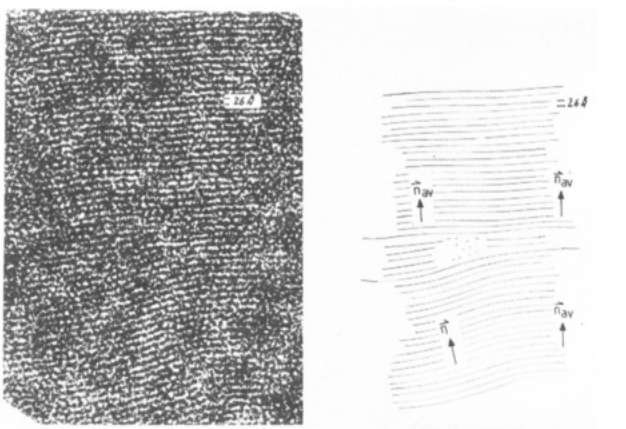

Figure 8. High-resolution image of a main-chain/side-group liquid crystalline polymalonate showing edge dislocation (5:2).

The undulating nature of the planes is still evident. In the vicinity of the defect, the director changes its average direction by an angle ϕ in order to accommodate one extra atomic plane.

The change in director direction becomes more obvious in the 4:2 (or 2:0) situation shown in Figure 7 where two additional planes are accommodated. As the difference p between incoming and outgoing smectic planes, i.e., the number of additional planes, increases, the value of ϕ increases. This is demonstrated in Figure 8–10 for p = 3–5, respectively.

Double Orientation

When thin films are investigated and translated under selected area diffraction conditions, a sudden change in

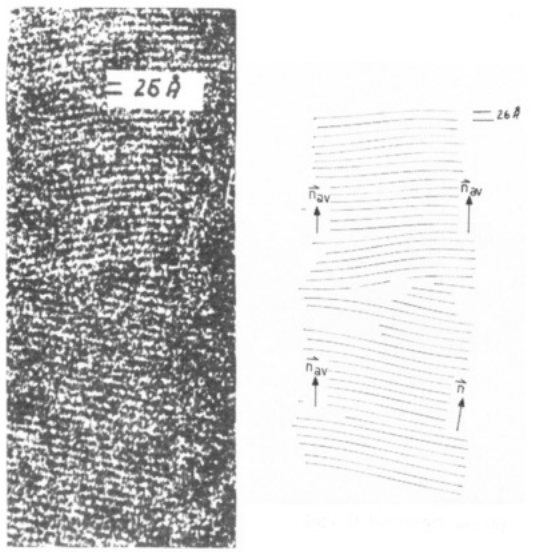

Figure 9. High-resolution image of a main-chain/side-group liquid crystalline polymalonate showing edge dislocation (4:0).

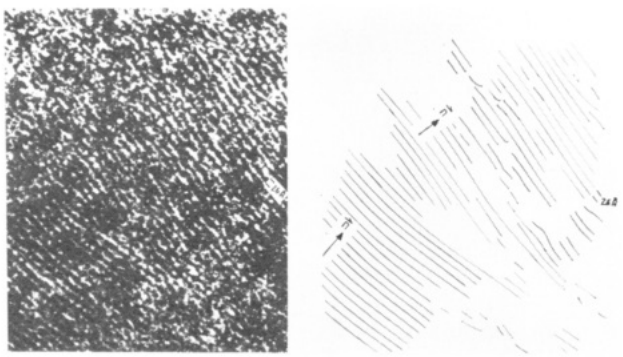

Figure 10. High-resolution image of a main-chain/side-group liquid crystalline polymalonate showing edge dislocation (6:1).

orientation of the diffraction pattern or, indeed, two different orientations simultaneously can sometimes be observed.

Figure 11 shows such an area. In the example of Figure 11, sets of smectic planes are shown to overlap. Each region forms its own set of undulating smectic planes. Such a micrograph showing cross-grating patterns, in addition to those showing undulations and defects, again proves conclusively that these micrographs do not show "artifacts" caused by astigmatism, etc., but real structural features.

Discussion

Indirect evidence suggesting that smectic planes in liquid crystals develop transverse oscillations in order to minimize the free energy has been presented previously.[6] In the cited example, analysis of the wave vector and intensity of satellite X-ray diffraction spots suggested a simple sinusoidal layer modulation with a wavelength of 78 ± 3 Å and an amplitude corresponding approximately to the interlayer spacing (<5 Å). In the case of liquid crystalline polymers, undulations are also observed, in this case, by direct observation in the electron microscope. However, wavelength, λ, and amplitude, a, are much larger. The difference between short-chain molecules and polymers is not surprising, in view of the fact that the repeat distances and elastic constants in the case of polymers are much larger. However, it is noteworthy that the amplitude corresponds approximately to the interlayer spacing in both cases.

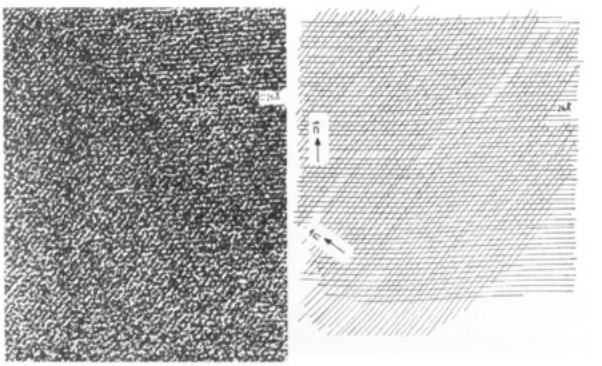

Figure 11. High-resolution image of a main-chain/side-group liquid crystalline polymer showing double orientation.

Coherent inelastic neutron scattering experiments on the short molecule liquid crystals[7] demonstrated this transverse wave to be a static, rather than dynamic, modulation (relaxation time, $<10^{-7}$ s). In view of the fact that the structures seen by electron microscopy were obtained by quenching the sample from the liquid into the solid state, the undulations observed in this work must represent a highly cooperative static modulation which develops during lateral growth in order to minimize the free energy of the system.

Theoretical calculations regarding the energetics of defects in liquid crystals have been discussed in detail recently.[8] It was shown that, while the defects in liquid crystals are topologically similar to their counterparts in crystals, they differ significantly from the point of view of energetics. For polymer systems, this will also apply. The aim of the present paper is not, however, a consideration of the free energy of elastic deformation, but rather an explorative study aimed at discovering and listing the nature of the defects which are formed. It has been shown that these systems develop single and multiple edge dislocations.

In order to gain a better understanding of these undulations and defects in smectics, a crystalline polymer system was studied; namely a polymer with an almost

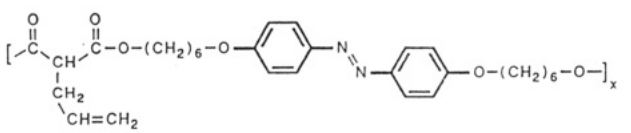

identical main-chain repeating unit but no side groups. The system was synthesized by Zentel and has been described elsewhere.[9] Thin films were oriented by shearing.

The electron diffraction pattern (Figure 12) indicates a highly crystalline structure with a small-angle maximum having 2 higher orders, giving a layer spacing L of 36 Å. In contrast to the main-chain/side-group polymer, this distance corresponds to the distance between mesogenic groups on the *fully extended chain*, as can be determined by model calculations using well-documented bond lengths.

The wide-angle maxima give d spacings of 3.8, 3.7, and 3.0 Å. The high resolution image (Figure 13) shows that the planes corresponding to the 36-Å spacing do not undulate in the manner discribed previously but are relatively straight over large distances.

There are, however, some characteristic features in the vicinity of defects. Figure 14 shows that boundaries in the lattice planes suddenly change direction. Only in the vicinity of dislocation are undulations observed. This is indicated in Figure 15, showing the undulations around three single edge dislocations marked D. Another demonstration of this feature is shown in Figure 16 where two

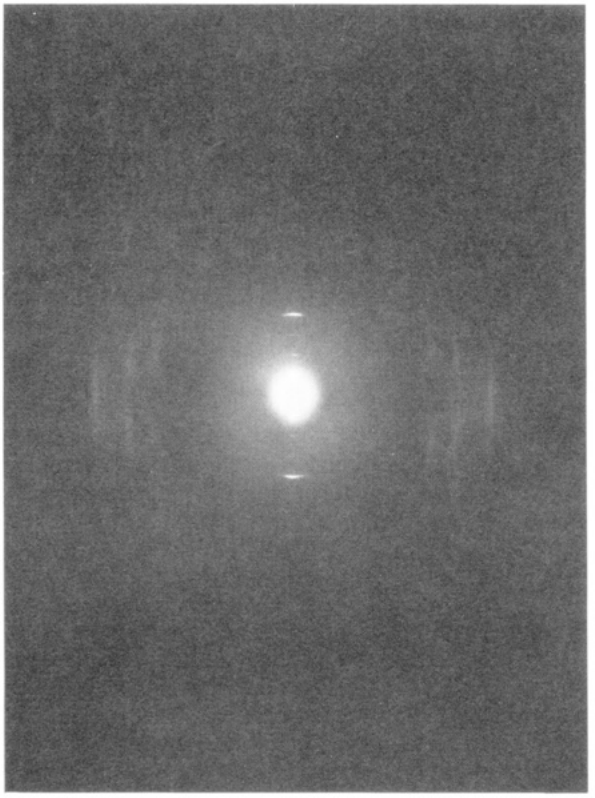

Figure 12. Diffraction pattern from a main-chain liquid crystal polymer (polymalonate with azobenzene as mesogenic group) in the crystalline phase.

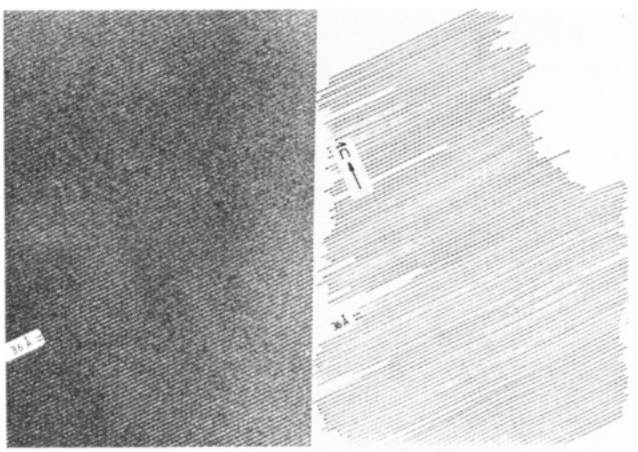

Figure 13. High-resolution image of a main-chain liquid crystal polymer (polymalonate with azobenzene as mesogenic group) in the crystalline phase.

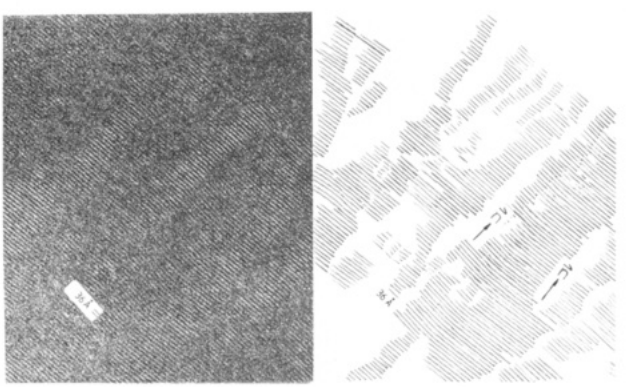

Figure 14. High-resolution image of a main-chain liquid crystal polymer (polymalonate with azobenzene as mesogenic group) in the crystalline phase showing small-angle boundaries.

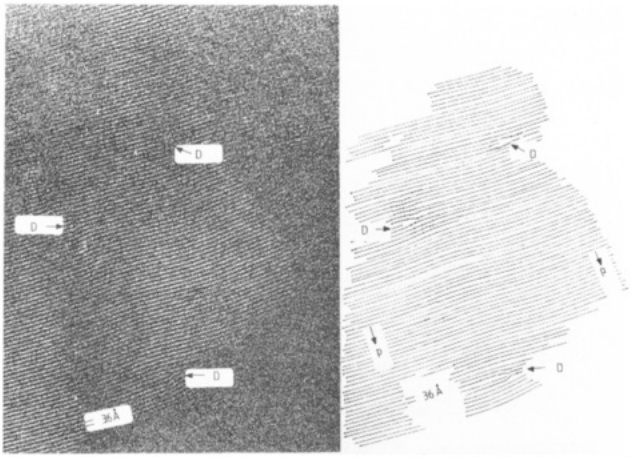

Figure 15. High-resolution image of a main-chain liquid crystal polymer (polymalonate with azobenzene as mesogenic group) in the crystalline phase indicating three edge dislocations.

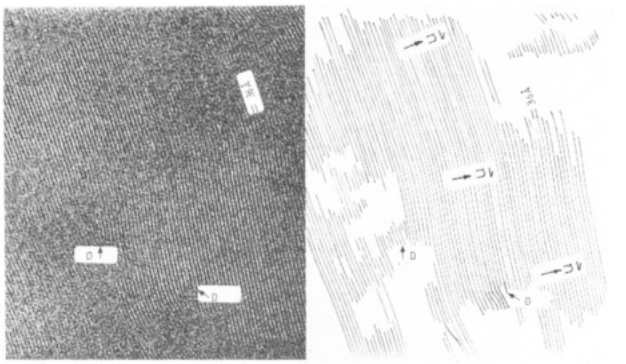

Figure 16. High-resolution image of a main-chain liquid crystal polymer (polymalonate with azobenzene as mesogenic group) in the crystalline phase indicating two edge dislocations.

dislocations are indicated and another must be situated in the region showing no contrast.

The experiment with the crystalline polymer has shown some very important differences and also similarities between the smectic and crystalline phases in these polymers:

The diffraction patterns appear to be entirely different. The long spacings differ, although the distance between mesogenic groups on the polymer chain is identical, and most important, the smectic structure gives a halo on the equator while the crystalline structure gives sharp reflections on the equator, indicating a fiber structure. In the crystalline phase, the spacings on the meridian correspond to the distance between mesogenic groups on the fully extended polymer chain, while the long spacings in the smectic phase are considerably shorter. This reduction arises because the side chains have to be accommodated, thus leading to a certain amount of disorder, which is, in fact, responsible for the formation of a liquid crystalline phase. However, these side chains are accommodated such that their mesogenic groups can be situated next to the mesogenic groups on the main chain if the polymer chain bends. Consequently, a smectic phase, rather than a nematic phase, develops. However, the halo shows that there is a considerable disorder between neighboring chains (i.e., d varies around 5Å). The high-resolution micrographs show that the smectic planes are rather "flexible": they undulate even in regions where there are no defects. Furthermore, a large number of additional smectic planes can be accommodated, leading to considerable distortion of the smectic planes. We know from the diffraction pattern that there is considerable disorder between layers. Furthermore, the dislocations which are observed are all

edge dislocations normal to the film.

The diffraction pattern from the polymer in the crystalline phase indicates that in this case the polymer chain is fully extended and that a fiber-type order is achieved in a direction perpendicular to this; i.e., there is order between the planes, giving rise the small-angle maxima. The high-resolution images indicate that these planes are relatively straight in the undisturbed regions but can accommodate an extra plane, giving on edge dislocation perpendicular to the film; this leads to considerable distortion of the atomic planes. Only edge dislocations of the 1:0 type were observed.

Therefore, although the electron diffraction patterns would indicate considerable differences between the two structures, the high-resolution micrographs show that there are surprising similarities in one well-defined direction. It also appears that details of molecular geometry are crucial in determining the structure and thus the phase which develops.

With regard to this investigation, the problems regarding the production and physical interpretation of phase contrast and the experimental conditions which are required to orientate the films and image smectic planes have been successfully solved. However, a major problem is still the low signal/noise ratio in the electron micrographs. This becomes particularly important when trying to discover the exact nature of the dislocation core and in deciding to what extent there is some orientation in the spaces between highly ordered regions after short annealing times. In a following paper, we describe approaches to this problem and the degree of success which has been achieved so far.

Acknowledgment. We are much indebted to Professor Sir Charles Frank for his very helpful and detailed comments on the original manuscript and to Professor H. Ringsdorf for giving us access to the beautiful samples synthesized in his department. We also acknowledge the admirable work of our photographer, E. R. Berger.

Registry No. Poly[oxy[2-[6-[4-[(4-cyanophenyl)azo]phenoxy]hexyl]-1,3-dioxo-1,3-propanediyl]oxy-1,6-hexanediyloxy-1,4-phenyleneazo-1,4-phenyleneoxy-1,6-hexanediyl], 97088-50-1; poly[oxy[1,3-dioxo-2-(2-propenyl)-1,3-propanediyl]oxy-1,6-hexanediyloxy-1,4-phenyleneazo-1,4-phenyleneoxy-1,6-hexanediyl], 105035-53-8.

References and Notes

(1) Reck, B.; Ringsdorf, H. *Makromol. Chem., Rapid Commun.* **1985**, *6*, 291.
(2) Voigt-Martin, I. G.; Durst, H. *Liq. Cryst.* **1987**, *2*, 585.
(3) Voigt-Martin, I. G.; Durst, H.; Reck, B.; Ringsdorf, H. *Macromolecules* **1988**, *21*, 1620.
(4) Erickson, H. P.; Klug, A. *Philos. Trans. R. Soc. London, B* **1971**, *B261*, 105.
(5) Voigt-Martin, I. G.; Durst, H. *Liq. Cryst.* **1987**, *2*, 601.
(6) Gane, P. A.; Leadbetter, A. J. *J. Phys. C* **1983**, *16*, 2059.
(7) Richardson, R. M.; Leadbetter, A. J.; Hayter, J. B.; Stirling, W. G.; Gray, G. W.; Tajbakhsh, A. *J. Phys. (Res Ulis, Fr.)* **1984**, *45*, 1061.
(8) Chandrasekhar, S.; Ranganath, G. S. *Adv. Phys.* **1986**, *35*, 507.
(9) Zentel, R.; Schmidt, G. F.; Meyer, J.; Benalia, M. *Liq. Cryst.* **1987**, *2*, 651.
(10) Voigt-Martin, I. G.; Durst, H.; Krug, H., submitted for publication in *Macromolecules*.

X-ray Photoelectron Spectroscopic and Theoretical Study of the Conformational Dependence of the Valence Electronic Levels in Hexagonal and Orthorhombic Poly(oxymethylenes)

P. Boulanger, J. Riga, J. J. Verbist,*,† and J. Delhalle‡

Laboratoire de Spectroscopie Electronique and Laboratoire de Chimie Théorique Appliquée, Facultés Universitaires Notre-Dame de la Paix, 61, rue de Bruxelles, B-5000 Namur, Belgium. *Received September 28, 1987; Revised Manuscript Received February 15, 1988*

ABSTRACT: X-ray photoelectron spectroscopy (XPS) valence band spectra of hexagonal and orthorhombic poly(oxymethylenes) are reported and compared with simulated XPS spectra based on ab initio calculations for simple model oligomers $CH_3O-(CH_2O-)_x-CH_3$ where $x = 1$, 3, 5, or 7. An attempt is made to interpret the observed differences as having a conformational origin.

Introduction

Because of its appropriate sampling depth compared to more classical spectroscopies, XPS (X-ray photoelectron spectroscopy) has been increasingly applied since 1972 to study fundamental structural questions and problems which arise at the surfaces and interfaces of technologically useful polymers. Interest was first focused on the core energy levels, which provide information on the chemical composition, bonding, and (in)homogeneity of the topmost atomic or molecular layers. However, a number of important problems have to do with the discrimination of possible differences between bulk and surface structural characteristics, the dependence of the latter on the bulk morphologies and preparation, etc.

To implement the description of the situation occurring at polymer surfaces and interfaces, it would be useful to obtain from the same XPS measurements some information about the molecular structure. Unfortunately, this is difficult to obtain from the core levels, which otherwise have the best resolution relative to the other parts of the spectrum.

As demonstrated in 1974 by quantum mechanical simulations and XPS spectra of model polymers,[1] the valence spectral data contain information on the primary and secondary structures of the polymer backbone. A few comparisons[2,3] between theoretically simulated and measured valence band spectra of pure hydrocarbon polymers have provided a basis for establishing relationships be-

† Laboratoire de Spectroscopie Electronique.
‡ Laboratoire de Chimie Théorique Appliquée.

0024-9297/89/2222-0173$01.50/0